Co-enhancing and -confining the electric and magnetic fields of the broken-nanoring and the composite nanoring by azimuthally polarized excitation

Ping Yu,[1] **Shuqi Chen,**[1,*] **Jianxiong Li,**[1] **Hua Cheng,**[1] **Zhancheng Li,**[1] **and Jianguo Tian**[1,2]

[1]*The Key Laboratory of Weak Light Nonlinear Photonics, Ministry of Education, School of Physics and Teda Applied Physics School, Nankai University, Tianjin 300071, China*
[2]*jjtian@nankai.edu.cn*
[*]*schen@nankai.edu.cn*

Abstract: We present a novel broken-nanoring, which can realize strongly localized confinement and highly enhancement for both electric and magnetic fields at two resonant modes excited by normal incident azimuthally polarized light. Two resonant modes of the broken-nanoring are formed by different resonant mechanisms as different resonant lengths. The physical model for two resonant modes is also proposed to explain the mechanisms of the electromagnetic enhancement. The enhancement of the electric and magnetic fields can be further improved by adding a nanoring at the outside of the broken-nanoring to form a composite nanoring, which can freely tune or easily merge the resonant modes of the solitary broken-nanoring while keeping larger enhancement of the electric and magnetic fields.

OCIS codes: (160.3918) Metamaterials; (240.6680) Surface plasmons; (260.2110) Electromagnetic optics; (260.5430) Polarization.

References and links

1. D. P. Fromm, A. Sundaramurthy, P. J. Schuck, G. Kino, and W. E. Moerner, "Gap-dependent optical coupling of single "bowtie" nanoantennas resonant in the visible," Nano Lett. **4**(5), 957–961 (2004).
2. N. Zhou, E. C. Kinzel, and X. Xu, "Complementary bowtie aperture for localizing and enhancing optical magnetic field," Opt. Lett. **36**(15), 2764–2766 (2011).
3. Z. Gao, L. Shen, E. Li, L. Xu, and Z. Wang, "Cross-diabolo nanoantenna for localizing and enhancing magnetic field with arbitrary polarization," J. Lightwave Technol. **30**(6), 829–833 (2012).
4. T. Grosjean, M. Mivelle, F. I. Baida, G. W. Burr, and U. C. Fischer, "Diabolo nanoantenna for enhancing and confining the magnetic optical field," Nano Lett. **11**(3), 1009–1013 (2011).
5. M. Lorente-Crespo, L. Wang, R. Ortuño, C. García-Meca, Y. Ekinci, and A. Martínez, "Magnetic hot spots in closely spaced thick gold nanorings," Nano Lett. **13**(6), 2654–2661 (2013).
6. T. H. Taminiau, R. J. Moerland, F. B. Segerink, L. Kuipers, and N. F. van Hulst, "$\lambda/4$ resonance of an optical monopole antenna probed by single molecule fluorescence," Nano Lett. **7**(1), 28–33 (2007).
7. C. Granata, E. Esposito, A. Vettoliere, L. Petti, and M. Russo, "An integrated superconductive magnetic nanosensor for high-sensitivity nanoscale applications," Nanotechnology **19**(27), 275501 (2008).
8. E. Vourch, P.-Y. Joubert, and L. Cima, "Analytical and numerical analyses of a current sensor using nonlinear effects in a flexible magnetic transducer," Prog. Electromagnetics Res. **99**, 323–338 (2009).
9. S. Kim, J. Jin, Y. J. Kim, I. Y. Park, Y. Kim, and S. W. Kim, "High-harmonic generation by resonant plasmon field enhancement," Nature **453**(7196), 757–760 (2008).

#193474 - $15.00 USD Received 8 Jul 2013; revised 11 Aug 2013; accepted 19 Aug 2013; published 27 Aug 2013

10. T. Schumacher, K. Kratzer, D. Molnar, M. Hecntschel, H. Giessen, and M. Lippitz, "Nanoantenna-enhanced ultrafast nonlinear spectroscopy of a single gold nanoparticle," Nat. Commun. **2**, 333 (2011).
11. M. W. Klein, C. Enkrich, M. Wegener, and S. Linden, "Second-harmonic generation from magnetic metamaterials," Science **313**(5786), 502–504 (2006).
12. M. L. Juan, M. Righini, and R. Quidant, "Plasmon nano-optical tweezers," Nat. Photon. **5**(6), 349–356 (2011).
13. K. Wang, E. Schonbrun, P. Steinvuzel, and K. B. Crozier, "Trapping and rotating nanoparticles using a plasmonic nano-tweezer with an integrated heat sink," Nat. Commun. **2**, 469 (2011).
14. M. W. Knight, H. Sobhani, P. Nordlander, and N. J. Halas, "Photodetection with active optical antennas," Science **332**(6030), 702–704 (2011).
15. H. Hong, H.-J. Krause, K. Song, and C.-J. Choi, "In situ analysis of free radicals from the photodecomposition of hydrogen peroxide using a frequency-mixing magnetic detector," Appl. Phys. Lett. **101**(5), 054105 (2012).
16. Y. Yang, H. T. Dai, and X. W. Sun, "Split ring aperture for optical magnetic field enhancement by radially polarized beam," Opt. Express **21**(6), 6845–6850 (2013).
17. G. M. Lerman, A. Yanai, and U. Levy, "Demonstration of nanofocusing by the use of plasmonic lens illuminated with radially polarized light," Nano Lett. **9**(5), 2139–2143 (2009).
18. J. Scheuer, "Ultra-high enhancement of the field concentration in split ring resonators by azimuthally polarized excitation," Opt. Express **19**(25), 25454–25464 (2011).
19. M. A. Suarez, T. Grosjean, D. Charraut, and D. Courjon, "Nanoring as a magnetic or electric field sensitive nano-antenna for near-field optics applications," Opt. Commun. **270**(2), 447–454 (2007).
20. E. D. Palik, *Handbook of Optical Constants of Solids* (Academic Press, 1998).
21. COMSOL 3.4, Comsol Multiphysics, http://www.comsol.com.
22. S. D. Liu, Z. S. Zhang, and Q. Q. Wang, "High sensitivity and large field enhancement of symmetry broken Au nanorings: effect of multipolar plasmon resonance and propagation," Opt. Express **17**(4), 2906–2917 (2009).
23. J. Li, S. Chen, P. Yu, H. Cheng, W. Zhou, and J. Tian, "Large enhancement and uniform distribution of optical near-field through combining periodic bowtie nanoantenna with rectangular nanoaperture array," Opt. Lett. **36**(20), 4014–4016 (2011).

1. Introduction

The development of metamaterials has led to the realization of phenomena that cannot be obtained with natural materials. A dramatic growth is witnessed in the researches of plasmonic structures, which can convert optical radiations into intense, engineered, and localized field distributions. The ability to focus and concentrate high optical intensities in ultra-small volumes and sub-diffraction limits of some nanostructures contains two aspects: electric confinement and magnetic confinement. It is well-known that high electric field enhancement and confinement are created in the air gap between two closely spaced metal nanoparticles [1]. This effect has long been exploited in the field of surface-enhanced Raman spectroscopy (SERS). Recently, more and more people start to research the properties to enhance and confine the magnetic field of the nanostructures [2–5]. The capability of some optical nanostructures to develop magnetic moments offers the possibility to locally enhance the magnetic near-field. These nanostructures can be used as detectors for the optical magnetic field and for the magneto-optic modulation. However, these efforts have only a study on the characteristics of electric or magnetic field under the scalar beams separately, which limit the flexibility and diversity of the structures in some applications. If we combine the study of electric and magnetic fields, the structures not only can be used more convenient, but also has more diverse applications in electromagnetic sensing [6–8], nonlinear optics [9–11], particle trapping [12, 13], detection [14, 15] and many more.

Recently, utilizing the vector beams to confine incident light into the nanometer scale has become a new focal point of research [16]. It was shown that highly symmetrical radially and azimuthally polarized light have much more advantages than scalar light. For instance, the vector beams can be coupled more efficiently to plasmonic lenses and produce brighter "hot-spot" than those produced by linearly polarized light [17]. Moreover, compared to linearly polarized illumination, the azimuthally polarized illumination increases the intensity enhancement by more than an order of magnitude in split-ring resonators (SRRs) [18]. Therefore, some researchers pay more attention to the interesting phenomenon generated by the vector beams. Suarez *et*

#193474 - $15.00 USD Received 8 Jul 2013; revised 11 Aug 2013; accepted 19 Aug 2013; published 27 Aug 2013

al. proposed that either the electric or the magnetic emission can be enhanced by the nanoring nanoantenna illuminated by the radial or azimuthal polarization, respectively [19]. However, they can not realize co-enhancement of electric and magnetic fields illuminated by the radial or azimuthal polarization, which can broaden the applications of electric and magnetic fields in nanoscale.

In this paper, we present a novel broken-nanoring, which can realize strongly localized confinement and highly enhancement for both electric and magnetic fields at two resonant modes excited by normal incident azimuthally polarized light. Two resonant modes of the broken-nanoring are formed by different resonant mechanisms as different resonant lengths in each mode, which result in different enhancement factors for electric or magnetic field. We also propose the physical model for two resonant modes to explain the mechanisms of the electromagnetic enhancement. The enhancement of the electric and magnetic fields can be further improved by adding a nanoring at the outside of the broken-nanoring to form a composite nanoring. Different nanorings can freely tune or easily merge the resonant modes of the solitary broken-nanoring while keeping larger enhancement of the electric and magnetic fields.

2. Co-enhancing and -confining the electromagnetic fields by broken-nanoring

A sketch of the proposed broken-nanoring is shown in Fig. 1. The broken-nanoring is fabricated onto a glass substrate and surrounded by air above. The design of the broken-nanoring can be described as a nanoring with a small gap. The radius r_1 and width w_1 of the nanoring are 100 nm and 30 nm, respectively. The thicknesses of the nanoring and the gap are given by t_0=60 nm and t_1=40 nm, and the gap length is defined by g=14 nm. We choose gold as the material of broken-nanoring and fit a Drude model with the relative permittivity at infinite frequency ε_∞=9.0, the plasma frequency $\omega_p = 1.3166 \times 10^{16}$ s^{-1}, and the damping constant $\gamma = 1.3464 \times 10^{14}$ s^{-1} [20]. The refraction index of the substrate is chosen to be equal to 1.5. All boundaries of the computation volume are terminated with perfectly matched layers (PMLs) in order to avoid parasitic unphysical reflections around the broken-nanoring. In order to calculate the electromagnetic response of the broken-nanoring under excitation with an azimuthally polarization light, the three-dimensional Finite Element Method (FEM) method is utilized by using COMSOL Multiphysics [21].

To observe the electric and magnetic resonance of the broken-nanoring illuminated by normal

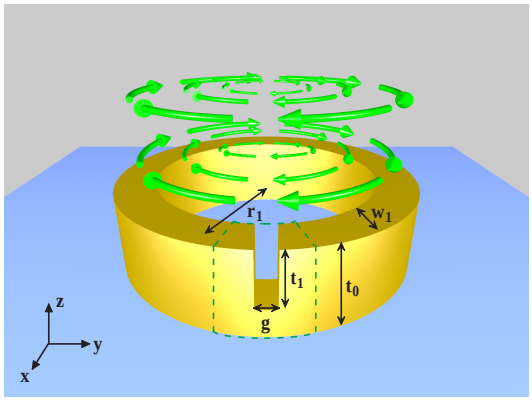

Fig. 1. Schematic illustration of the broken-nanoring, r_1=100 nm, w_1=30 nm, t_0=60 nm, t_1=40 nm and g=14 nm. The green arrows show the normal incident azimuthally polarized light.

#193474 - $15.00 USD Received 8 Jul 2013; revised 11 Aug 2013; accepted 19 Aug 2013; published 27 Aug 2013

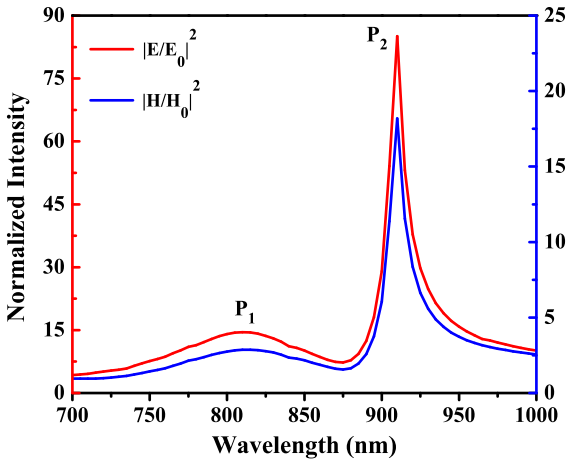

Fig. 2. Calculated normalized intensity spectra of the broken-nanoring for electric (red line) and magnetic (blue line) fields.

incident azimuthally polarized light, we gave the normalized intensity spectra of both electric and magnetic fields in Fig. 2. The normalized intensity spectrum of electric or magnetic field exhibits two distinct resonant peaks. Meanwhile, the resonant wavelengths of electric or magnetic field are totally superposition at P_1=810 nm and P_2=910 nm, respectively. The intensity enhancement at two resonant peaks can be clearly observed, especially for P_2. The normalized intensity we defined is the maximum electric or magnetic field intensities in the transverse plane through the center of the gap region along *z* direction at each wavelength normalized by the intensities calculated at the same plane without the presence of any nanostructure.

3. Physical mechanisms for co-enhancing and -confining the electromagnetic fields

In order to analyze the confined characteristics of the electric and magnetic fields for the presented broken-nanoring, we calculated the localized near-field distributions of the electric and magnetic fields at two main resonant wavelengths in Fig. 3. Intensity plots are given along the transverse (*x*-*y*) and the longitudinal (*x*-*z*) planes. The *x*-*y* plane is taken at the middle of the gap region along *z* direction whereas the *x*-*z* plane crosses the center of the broken-nanoring. As depicted in Figs. 3(a) and 3(b), the hot spot of the electric field generated by the broken-nanoring is concentrated in nanoscale at the gap region either in *x*-*y* or in *x*-*z* plane. This effect becomes gradually weak at the wavelengths away from these two resonant wavelengths as shown in Fig. 3(c). As depicted in Figs. 3(d) and 3(e), the distributions of magnetic field at two resonant wavelengths in *x*-*y* or in *x*-*z* plane almost have the same vision with those of electric field. Though the maximal intensity position of magnetic near-field is not completely overlapped with that of electric near-field, the large magnetic enhancement still appears at the gap region. However, we almost can not find the magnetic field confined in the gap region at 740 nm as shown in Fig. 3(f), while only the electric field could be observed. These provide the clear evidence that the electric and magnetic fields can be strongly localized and highly enhanced at the gap region under the same resonant wavelength for the proposed broken-nanoring.

Two resonant modes of the broken-nanoring excited by normal incident azimuthally polarized light have different forming mechanisms, which can result in different enhancement factors

#193474 - $15.00 USD Received 8 Jul 2013; revised 11 Aug 2013; accepted 19 Aug 2013; published 27 Aug 2013

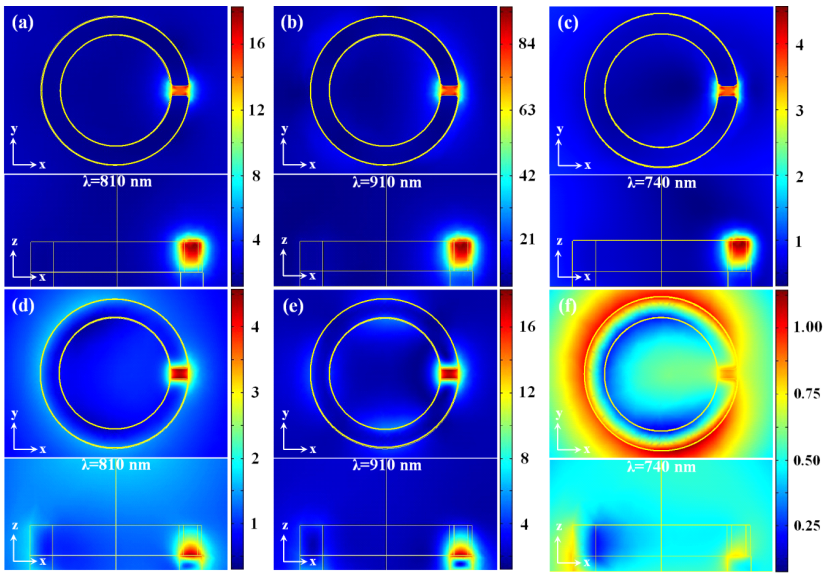

Fig. 3. Calculated normalized near-field distributions of the broken-nanoring for electric fields at (a) mode 1, (b) mode 2, (c) 740 nm, and magnetic fields at (d) mode 1, (e) mode 2, (f) 740 nm in *x*-*y* and *x*-*z* planes, respectively. The cutting planes are all through the middle of the gap region.

for electric or magnetic field. To clearly observe the resonant region, we calculated the electric near-field distributions in logarithmic scale in *x*-*y* plane and in *y*-*z* plane at two resonant wavelengths, respectively. There is no obviously resonance along the circle ring in *x*-*y* plane for mode 1, as shown in Fig. 4(a). This mode is formed by the resonance of U-shaped region as shown in Fig. 4(b), which has been indicated in dashed line in Fig. 1. The mode 2 is from the resonance of the broken-nanoring, which can be confirmed from the electric near-field distributions in Figs. 4(c) and 4(d). This kind of resonant mode is analogous to the appearance of quadruple plasmon mode in the nanoring structure [22]. It has a sufficient resonant effect caused by the advisable interaction between the broken-nanoring and the incident azimuthally polarization so that the normalized intensity for both electric and magnetic fields of mode 2 is larger than that of mode 1. Therefore, the intensity difference between the two resonant wavelengths arises from the different resonant lengths in each mode. Since the analysis method of magnetic resonant modes is similar to that of the electrical resonant modes, we only investigate the resonant mechanisms of the electrical resonant modes.

To further analyze the enhanced mechanisms of electromagnetic field for two resonant modes, we gave the physical model for two resonant modes and field distributions for electric and magnetic fields in Fig. 5. As mentioned before, the resonance of mode 1 happens in the U-shaped region. It therefore can provide currents to form resonant current loop as the green lines indicated in Fig. 5(a). The gap between the metallic strips introduces capacitance and the current loop introduces inductance. Following Ampere's law, the resulting of increasing the current intensity leads to an enhancement of the magnetic field as the blue arrows indicated. Not all of the charges can transfer through the junction between the side edges of the broken-nanoring to generate magnetic field. Part of the charges will accumulate on the side edges of the broken-nanoring leading to the enhancement of electric field in gap region. The normal incident azimuthally polarized light mainly excites and accumulates the charges on two end faces of the

#193474 - $15.00 USD Received 8 Jul 2013; revised 11 Aug 2013; accepted 19 Aug 2013; published 27 Aug 2013

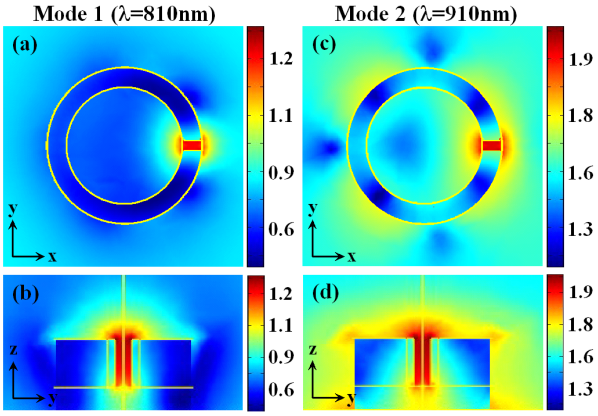

Fig. 4. Calculated normalized electric near-field distributions in logarithmic scale (a), (c) in *x-y* plane and (b), (d) in *y-z* plane at two resonant wavelengths, respectively.

broken-nanoring for the resonance of mode 2, as shown in Fig. 5(b). Therefore, the strong electric field enhancement occurs in the gap region indicating by the red arrows. Furthermore, the charges can transfer towards the connection between two end faces. The two end faces of the broken-nanoring not only act as an electric funnel, but also reinforce the optical current density into the junction, leading to a large magnetic field enhancement in the gap region. Thus, the simultaneous enhancement of the electric and magnetic fields exists in the gap region for both mode 1 and mode 2. Meanwhile, we calculate the corresponding instantaneous magnetic and electric distributions in *x-y* plane for mode 1 [Fig. 5(c)] and mode 2 [Fig. 5(d)], respectively. The longer arrows represent the stronger intensity. The simulated results of two resonant modes are in good agreement with those of theoretical prediction. This enhanced mechanism

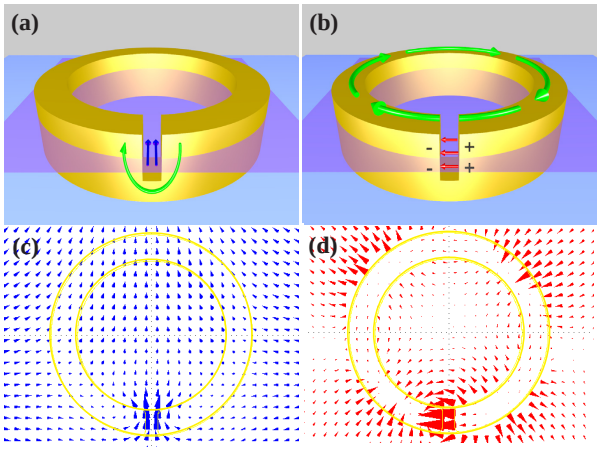

Fig. 5. Physical model for the resonance of (a) mode 1 and (b) mode 2. Numerical simulations of instantaneous (c) magnetic distributions at mode 1 and (d) electric distributions at mode 2. The cross-sections in (c) and (d) are indicated by the pink planes along the middle of the gap region of the broken-nanoring in (a) and (b). Blue and red arrows represent the orientations of magnetic and electric fields at instantaneous time, respectively.

#193474 - $15.00 USD Received 8 Jul 2013; revised 11 Aug 2013; accepted 19 Aug 2013; published 27 Aug 2013

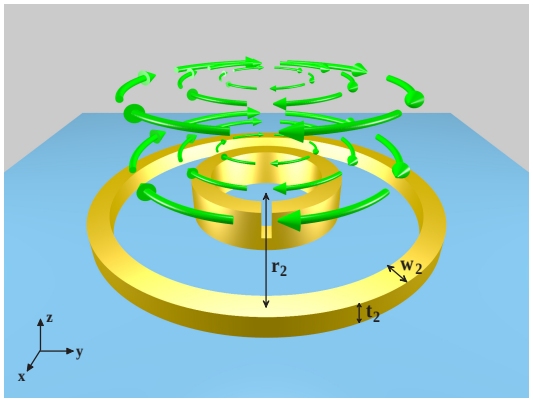

Fig. 6. Schematic illustration of the composite nanoring. The radius, thickness and width of the outside nanoring are denoted by r_2, t_2 and w_2, respectively.

can be extended to other conventional or unconventional light polarizations by designing different nanostructures.

4. Further Co-enhancing the electromagnetic fields by composite nanorings

In order to further enhance the electric and magnetic fields, we added a nanoring at the outside of the broken-nanoring to form a composite nanoring, which is shown in Fig. 6. We firstly optimized geometry parameters of the nanoring to separately enhance two resonant modes of

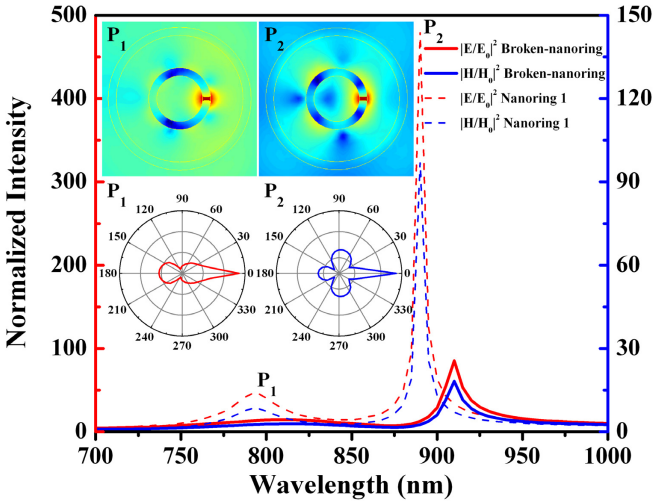

Fig. 7. Normalized intensity spectra of both electric and magnetic fields for the composite nanoring (dotted line) and broken-nanoring (solid line) illuminated by azimuthally polarized light. Insets: normalized electric near-field distributions and the corresponding numerical value distributions in *x*-*y* plane in logarithmic scale for the composite nanoring at two resonant modes.

#193474 - $15.00 USD Received 8 Jul 2013; revised 11 Aug 2013; accepted 19 Aug 2013; published 27 Aug 2013

the broken-nanoring. Figure 7 gives the normalized intensity spectra of both electric and magnetic fields for the composite nanoring and broken-nanoring illuminated by azimuthally polarized light. The normalized standard of the composite nanorings is same with that of broken-nanoring. The radius, thickness and width of the nanoring are fixed at r_2=250 nm, t_2=15 nm and w_2=30 nm, respectively. It has been shown that the composite nanoring can modify the resonant wavelengths and exhibit larger field enhancement than that of the broken-nanoring. The resonant peaks have a 20 nm redshift compared with that of the broken-nanoring due to the coupling of each other. Meanwhile, the electric and magnetic fields of the composite nanoring are still assembled in the gap region of the broken-nanoring and retain a nanoscale volume as expected. The normalized electric near-field distributions and the corresponding numerical value distributions in *x-y* plane in logarithmic scale for the composite nanoring at two resonant modes are shown in the insets of Fig. 7, respectively. The electric near-field distributions and numerical value distributions in *x-y* plane at two resonant modes illustrate that two different resonant modes still exist separately. The difference between two resonant modes can be more obviously observed. The large near-field enhancement can be explained by the double interaction between the composite nanoring and azimuthally polarized light [23]. First, the incident azimuthally polarized light is interacted with the nanoring. The nanoring can allow more efficient concentrating and focusing of the beam power. Then, the concentrated near-field in nanoring has been further enhanced by broken-nanoring, which results in a large near-field enhancement for the composite nanoring. It is these capacities of both two single nanorings that make the composite nanoring realize a larger enhancement than that of the solitary broken-nanoring.

To improve the performances of the electric and magnetic fields enhancement for composite nanoring, we adjust the geometry parameters of the nanoring to merge two resonant modes of broken-nanoring. Figure 8 shows the spectral responses for the second composite nanoring and

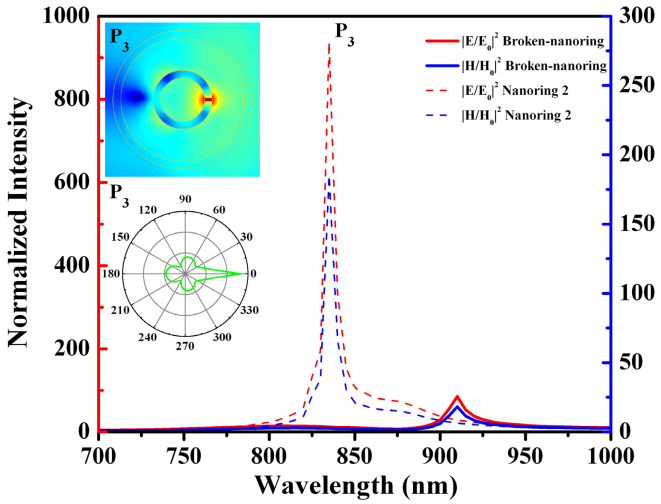

Fig. 8. Normalized intensity spectra of both electric and magnetic fields for the second composite nanoring (dotted line) and broken-nanoring (solid line) illuminated by azimuthally polarized light. Insets: normalized electric near-field distributions and the corresponding numerical value distribution in *x-y* plane in logarithmic scale for the second composite nanoring at the mixed resonant mode.

#193474 - $15.00 USD Received 8 Jul 2013; revised 11 Aug 2013; accepted 19 Aug 2013; published 27 Aug 2013

broken-nanoring. The radius, thickness and width of the second nanoring are r_2=225 nm, t_2=5 nm and w_2=30 nm, respectively. The second composite nanoring can induce larger electric and magnetic fields enhancement at P_3=835 nm comparing with the solitary broken-nanoring or first composite nanoring. To reveal the differences of the enhanced mechanism between these two composite nanorings, we also calculate the normalized electric near-field distributions and the corresponding numerical value distributions in *x*-*y* plane in logarithmic scale for the second composite nanoring, as shown in the insets of Fig. 8. Logarithmic scaled near-field distributions distinctly show the transitional state between the two kinds of resonant modes. It is not merely to enhance any of the single resonant modes, but rather the mix of two modes. The numerical value distribution also demonstrates the resonance at P_3 is a mixture of two resonant modes, because of the intensity numerical value distribution has the characteristics of both two modes. This outstanding property of large enhancing the electric and magnetic fields may lead this composite nanoring to the more widely applications.

5. Conclusion

In conclusion, we have presented a broken-nanoring to realize strongly localized confinement and highly enhancement for both electric and magnetic fields illuminated by azimuthally polarized light. Two different enhancement factors for electric and magnetic fields can be obtained as different resonant modes of the broken-nanoring. To improve the performances of the electric and magnetic fields enhancement for the broken-nanoring, we have added a nanoring at the outside of the broken-nanoring to form a composite nanoring, which can freely tune or easily merge the resonant modes of the solitary broken-nanoring. The property of highly co-enhancing both electric and magnetic fields is significant important for the applications of particle trapping and acceleration by using vector beams, since this ability can well increase the rate of particle trapping and improve the sensitivity of particle manipulating. Meanwhile, it is also highly expected to be useful in a wide range of optical detection, electromagnetic sensing, nonlinear optics and any more. The presented effect also plays an important role in improving the properties of SRRs. Previous studies on SRRs pay more attention to the electric modes analysis or the electric field enhancement at the split region. The presented effect also fills the vacancy of the co-enhancing and -confining electromagnetic fields.

Acknowledgments

This work was supported by the National Basic Research Program (973 Program) of China (2012CB921900), the Chinese National Key Basic Research Special Fund (2011CB922003), the Natural Science Foundation of China (61008002), the Natural Science Foundation of Tianjin (13JCQNJC01900), the Specialized Research Fund for the Doctoral Program of Higher Education (20100031120005 and 20120031120032), the Fundamental Research Funds for the Central Universities, and the 111 project (B07013).

#193474 - $15.00 USD Received 8 Jul 2013; revised 11 Aug 2013; accepted 19 Aug 2013; published 27 Aug 2013